Available online at www.sciencedirect.com
SCIENCE DIRECT®
ELSEVIER
Bioorganic & Medicinal Chemistry 12 (2004) 1467–1474
Bioorganic & Medicinal Chemistry

Further insights on the structural aspects of PLA_2 inhibition by γ-hydroxybutenolide-containing natural products: a comparative study on petrosaspongiolides M–R

Maria Chiara Monti, Agostino Casapullo, Raffaele Riccio and Luigi Gomez-Paloma*

Dipartimento di Scienze Farmaceutiche, Università di Salerno, via Ponte Don Melillo, 84084, Fisciano (SA), Italy

Received 15 July 2003; accepted 22 December 2003

Abstract—Petrosaspongiolides M–R (PM–PR, **1**–**5**) are marine sesterterpenes structurally characterised by a γ-hydroxybutenolide moiety. They have shown an in vitro and in vivo potent anti-inflammatory activity, mediated by specific inhibition of secretory phospholipase A_2 (*s*PLA_2 enzymes). The molecular mechanism underlying the sub-micromolar irreversible inhibition of the bee-venom PLA_2 (*bv*PLA_2) by PM has been clarified combining mass spectrometry (MS) and molecular modelling approaches. The N-terminal amino group (Ile-1 residue), recently identified as the unique PM covalent binding site on this enzyme, selectively delivers a nucleophilic attack onto the masked aldehyde at C-25 of the pharmacophoric γ-hydroxybutenolide ring of PM, giving rise to a Schiff base. In the attempt of broadening the knowledge of the mechanism at molecular level of PLA_2 inactivation by this family of compounds, we performed a comparative analysis on petrosaspongiolides M-R, whose results are discussed in this paper. Firstly, the amount of *bv*PLA_2 enzyme covalently modified after incubation with each of petrosaspongiolides M-R was measured and resulted to be in good agreement with pharmacological in vitro data. Then, a full characterisation of the *bv*PLA_2 adduct with PR, one of the least active and most structurally different among petrosaspongiolides, by LC-MS, MS^n, and computational methods, confirmed the same inhibition mechanism and covalent binding site already found for PM. Finally, extensive molecular docking studies performed in comparison on the PM–PLA_2 and PR–PLA_2 complexes provided critical insight on how the balance between non-covalent and covalent inhibitor-enzyme interactions may affect the final potency exhibited by the various compounds of the petrosaspongiolide family.

1. Introduction

A number of marine metabolites are known to possess anti-inflammatory activity. In particular, many marine terpenoids have recently shown the ability to interfere with the complex network of biochemical pathways connected to inflammation processes.[1]

In the course of our investigations on the chemistry and biology of pharmaceutically active compounds from natural sources, we have recently focused our attention on PM (**1**) (Fig. 1), a γ-hydroxybutenolide-containing sesterterpenoid isolated from the New Caledonian marine sponge *Petrosaspongia nigra*, along with a series of related products (PN–PR, **2**–**5**).[2] All of them share the pharmacophoric γ-hydroxybutenolide ring, the structural unit responsible for their irreversible inhibitory activity toward group II and III secretory phospholipase A_2 (PLA_2) enzymes, such as bee venom, *Naya naya* and human synovial PLA_2 preparations.[2,3]

Among them, PM (**1**) has been the subject of a detailed in vitro and in vivo pharmacological investigation.[4] PM shows an IC_{50} of 0.6 μM toward bee venom PLA_2 [for comparison manoalide (MLD), considered the reference compound within this class of natural products, displays an IC_{50} of 7.5 μM in the same conditions].[2,5] It is able to reduce in a dose-dependent manner the levels of various pro-inflammatory mediators, such as prostaglandin E_2 (PGE_2), tumor necrosis factor α (TNFα), and leucotriene B_4 (LTB_4)[4] and it has shown to modulate the expression of inducible cyclooxygenase and nitric oxide synthetase (COX-2 and iNOS) by interfering with the nuclear factor κB (NF-κB) pathways, thus

Keywords: Anti-inflammatory compounds; Marine natural products; Mass spectrometry; Phospholipase A_2 inhibition.
* Corresponding author. Tel.: +39-089-962811; fax: +39-089-962828; e-mail: gomez@unisa.it

0968-0896/$ - see front matter © 2004 Elsevier Ltd. All rights reserved.
doi:10.1016/j.bmc.2003.12.038

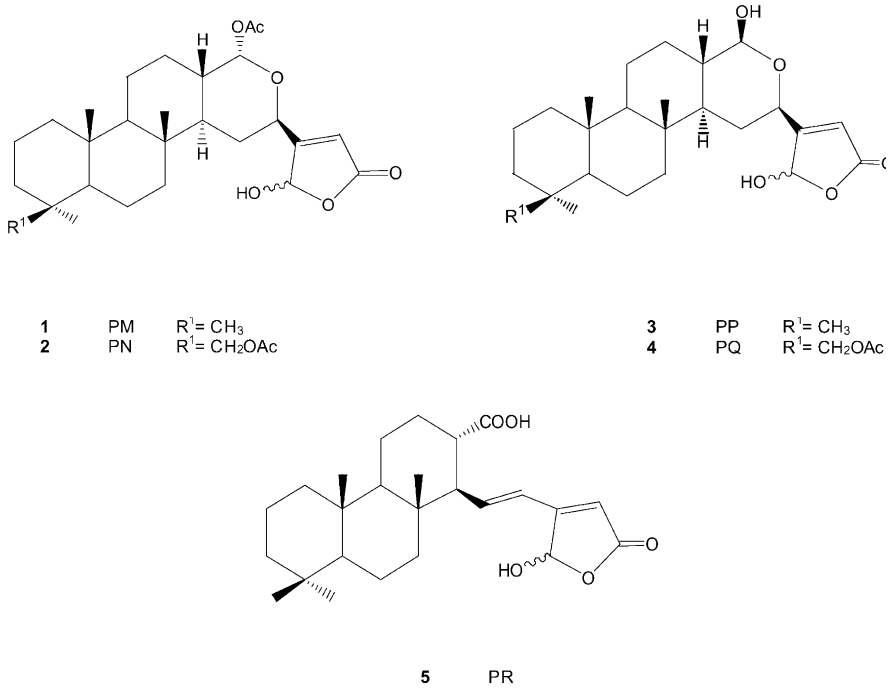

1 PM $R^1 = CH_3$
2 PN $R^1 = CH_2OAc$
3 PP $R^1 = CH_3$
4 PQ $R^1 = CH_2OAc$
5 PR

Figure 1. Chemical structures of petrosaspongiolides M–R (**1**–**5**).

decreasing NF-κB-DNA binding in response to zymosan, in mouse peritoneal macrophages.[6] This study also indicated that PM could interfere with a key step in NF-κB activation, the phosphorylation of IκBα, resulting in inhibition of IκBα degradation. The control of such a wide range of mediators by PM suggests a remarkably wide therapeutic spectrum for this marine metabolite in inflammatory conditions. Moreover, PM shows no significant side effects on gastric mucosa at 10 mg/kg and is orally administerable,[4] indicating that this molecule may constitute a useful model for the development of new agents for the treatment of acute and/or chronic inflammation. In fact, PLA_2, lying at the very top of the arachidonic acid cascade, is considered a particularly relevant pharmaceutical target.[7–15]

Interestingly, although the current medical practice includes many anti-inflammatory drugs modulating PLA_2 activity, notably corticosteroids, none of them are direct PLA_2 inhibitors.

The present study was planned to strengthen the previously proposed mechanism of interaction between PM and *bv*PLA_2[16] and to extend this mode of action to the related petrosaspongiolides. Moreover, the comparative analysis on the whole petrosaspongiolide family allowed a better comprehension at molecular level of the recognition processes regulating the inhibitor–enzyme interaction.

2. Results and discussion

In the present investigation, our attention was focused on three different aspects of the ligand-enzyme interaction, which required different experimental tools: (1) analysis by LC-MS of enzyme inactivation by petrosaspongiolides M–R and comparison of the results with inhibition data of in vitro assays; (2) identification on *bv*-PLA_2 of the punctual site of interaction of PR by proteolysis and LC-MS; (3) generation and comparison of PR and PM-PLA_2 adduct 3D models by molecular modelling approaches, using our experimental results as logical constraints to the calculations.

2.1. *Bv*PLA_2-petrosaspongiolides M–R complexes: a comparative analysis

Covalent complexes of petrosaspongiolides and *bv*PLA_2 were prepared, as previously described[16] (see also Experimental), separately adding the five inhibitors (PM, PN, PP, PQ, PR) to a solution of *bv*PLA_2 and incubating for 5 min at 40 °C with a 5:1 molar excess of individual petrosaspongiolides. Then, treatment with excess $NaBH_4$ afforded the selective reduction of the Schiff base formed during the incubation, as depicted in the reaction mechanism of Scheme 1. After quenching the reactions with an HCl 6M solution, the mixtures were chromatographed by RP-HPLC and the fractions collected were analysed by electrospray mass spectrometry (ESIMS). All the chromatograms were characterised by the presence of two main peak clusters, corresponding to unreacted protein (with one or two ox-Met residues) and monomodified protein species, respectively, as confirmed by ESIMS analysis (Table 1). The fraction of unreacted PLA_2 species was then used for the evaluation of the extent of inhibition of *bv*PLA_2. Accordingly, the areas of HPLC peaks relative to the intact protein species before and after incubation with each inhibitor were computed by integration and the percentage of petrosaspongiolide covalently modified protein was calculated by means of the following ratio:

$$\%\ \text{Binding} = \frac{\text{Area } bv\text{PLA}_2 \text{ peaks } prior \text{ incubation} - \text{Area } bv\text{PLA}_2 \text{ peaks } after \text{ incubation}}{\text{Area } bv\text{PLA}_2 \text{ peaks } prior \text{ incubation}} \times 100$$

The results obtained in this HPLC-MS analysis were then compared with the percentages of $bv\text{PLA}_2$ inhibition at 10 μM, previously measured by standard in vitro enzymatic assays,[2] showing a relatively good correlation profile (Fig. 2). In particular, if individual absolute IC_{50} values are not perfectly reproduced by our HPLC-MS data on modified PLA_2 species, a remarkable analogy may be noted in the relative trend of reactivity among the different agents. The similar pattern of the two sets of data of Figure 2 may be considered, in our opinion, an evidence in support of the proposed molecular mechanism of covalent modification of $bv\text{PLA}_2$ as the sole chemical event causing the inactivation of the enzyme, and ultimately, biological activity. Moreover, we took these results also as validation of the experimental design of our incubation procedure.

2.2. Structural characterisation of PR–PLA_2 adduct

In order to further validate and extend to the whole family of petrosaspongiolides M–R the inhibition model proposed for PM,[16] we submitted PR, the most structurally different and one of the least active among this class of natural compounds, to reaction with $bv\text{PLA}_2$, using similar experimental procedures as reported for PM.[16]

HPLC analysis of the reaction mixture after incubation of PR with $bv\text{PLA}_2$ and treatment with $NaBH_4$ gave fractions containing the unreacted protein and the PR–$bv\text{PLA}_2$ monomodified complex, as confirmed by ESIMS analysis (Fig. 3; molecular weight of unreacted protein = 16142.5 Da, molecular weight of monomodified complex = 16542.6 Da, mass difference = 400.1 Da). The HPLC purified $bv\text{PLA}_2$ fractions were subsequently subjected to disulfide bond reduction with DTT (dithiothreitol) (37 °C for 2 h) and alkylation of free cysteynil groups with iodoacetamide (rt for 45 min). After quenching the reaction, intact and covalently modified PLA_2 species were purified by RP-HPLC, and then submitted to extensive proteolysis experiments with endoproteinase Lys-C, which selectively cleaves peptide bonds at the C-terminus of Lys residues. The reaction was kept for 4 h at 37 °C, with a 1/50 (w/w) enzyme/substrate ratio. Digested peptides were eluted by RP-HPLC. Comparison between HPLC traces of digestion mixtures relative to intact and covalently modified PLA_2, led us to easily identify the points of difference. The following ESIMS analysis of digested peptides allowed us to unequivocally locate the covalent modification of PR on the N-terminal glycopeptide (1–14 residue), on the basis of the mass difference of 400 Da between the modified and unmodified peptide fragments (Table 2). This data confirmed the presence of a homogeneous monomodified PLA_2 species and established the location of the binding site for PR on the amino group of Ile-1 residue. It should be mentioned that the ε-amino group of Lys-14 residue may, at least in principle, represent another reactive site in the 1–14 peptide fragment, even if its implication is not consistent with the efficient performance of the endoproteinase Lys-C in cleaving the 14–15 peptide bond, as suggested by comparing the cleavage maps of the unmodified and modified PLA_2 species.

However, since the use of this kind of indirect argument left unsettled the same question in the PM-PLA_2 study too, we performed an ESIMS/MS analysis of the modified 1–14 peptide residue in order to get conclusive data on this matter. Thus, the collisionally activated 1–14 peptide fragment showed in the MS/MS spectrum strong b_{13} and b_{12} fragment ions, corresponding to the

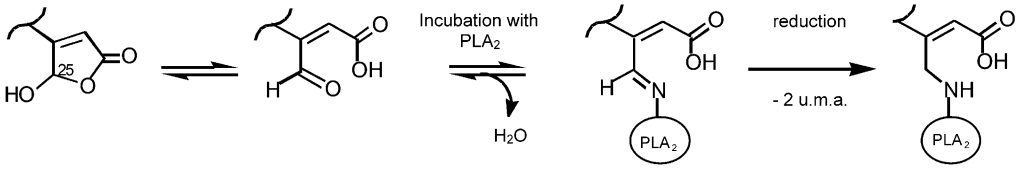

Scheme 1. Postulated mechanism for the inactivation of $bv\text{PLA}_2$ by petrosaspongiolides. The leak of one molecule of H_2O and the increment of 2 a.m.u. after $NaBH_4$ incubation were measured for each petrosaspongiolide by ESMS.

Table 1. Mass spectrometry analysis of $bv\text{PLA}_2$–Petrosaspongiolides adducts

Inhibitor and its MW	MW bvPLA$_2$[a]	MW of 1:1 complex after $NaBH_4$ treatment	Δ MW	MW of 2:1 complex after $NaBH_4$ treatment
PM (460Da)	16144.9 Da	16588.6 Da	443.7	17031.7 Da
PN (518Da)	16145.3 Da	16646.9 Da	501.6	17149.8 Da
PP (418Da)	16144.2 Da	16545.7 Da	401.5	16949.5 Da
PQ (476Da)	16145.0 Da	16606.5 Da	461.5	Nd
PR (416Da)	16142.8 Da	16542.6 Da	399.8	Nd

[a] Molecular weight (MW) of unreacted and modified glycoproteins is referred to most abundant isoform.

loss of Lys-14 and Asp-13 residues, respectively, from the C-terminus of the peptide (Fig. 4). These evidences indicated that the Lys-14 residue was unmodified, leading us to unambiguously assign the covalent modification of PLA_2 by PR on the amino group of Ile-1 residue. Overall, the experimental results obtained in the present study were equivalent to those reported for the PM and MLD agents, providing a strong indication of a common mechanism for the *bv*PLA_2 inhibition by γ-hydroxybutenolide-containing molecules.

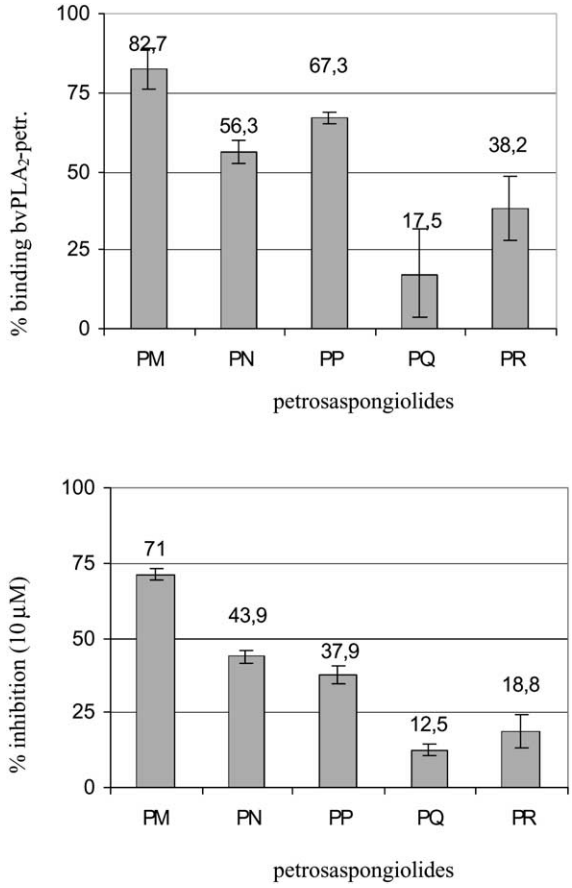

Figure 2. Upper panel: percentage data of reacted PLA_2 protein with each petrosaspongiolide (see Experimental). Lower panel: percentage data of inhibition at 10 μM measured in vitro pharmacological experiments.[2]

2.3. Docking studies of PM and PR molecules onto *bv*PLA_2

Extensive docking studies were performed on PM-*bv*PLA_2 and PR-*bv*PLA_2 complexes with the aim of getting refined models as tools for understanding the structural basis for the difference in activity displayed by these agents. Above all, we were interested in gaining more insight on how the fine balance between non-covalent interactions and chemical reactivity should affect their final biological activity. In fact, we reasoned that since all petrosaspongiolides share the same pharmacophoric γ-hydroxybutenolide moiety, their different efficiency in *bv*PLA_2 inhibition should not arise from intrinsic differences in reactivity of the individual mole-

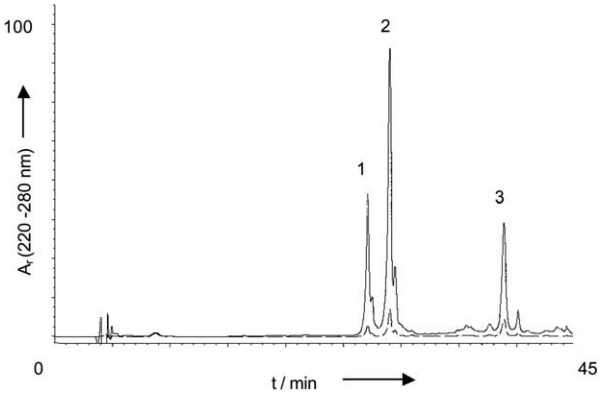

Figure 3. RP-HPLC separation of *bv*PLA_2–PR reaction products. Peak 1 corresponds to *bv*PLA_2 with 2 oxidized Met residues, peak 2 corresponds to *bv*PLA_2 with 1 oxidized Met residue and peak 3 corresponds to the 1:1 adduct between *bv*PLA_2 and petrosaspongiolide R.

Table 2. Mass spectrometry analysis of peptide maps of *bv*PLA_2 and *bv*PLA_2–PR after digestion by endoproteinase Lys C

Fraction	Measured mass (Da)	Peptide	Theoretical mass (Da)	bvPLA_2[a]	bvPLA_2R[a]
1	2188.44	48–66	2188.34	✓	✓
2	2582.20,	26–47 ox	2581.84,	✓	✓
	2189.65	48–66	2188.34	✓	
3	2566.04,	26–47	2565.84,	✓	✓
	844.50	67–72	844.98	✓	
4	2716.03	98–120	2715.01	✓	✓
5	1191.60	15–25	1191.31	✓	✓
6	2507.24,2669.65, 2654.00,2345.89	1–14 glycof.	2507.87,2671.87, 2653.87,2345.87	✓	
7	1388.90	73–85	1388.49	✓	✓
8	1161.0	86–94 ox	1159.37	✓	✓
9	1255.30	125–133	1254.95	✓	✓
10	1144.05	86–94	1143.37	✓	✓
11	1418.75	125–134	1418.0	✓	✓
12	2907.55,3069.56, 3054.56,2746.03	1–14 glycof.modified by PR	2907.87,3071.87, 3053.87,2745.87		✓

[a] Check marks indicate that the corresponding peptides were found in the digested mixture.

cules. More likely, highly influential on the overall inhibitory activity are either their (different) PLA_2 non-covalent affinity at the molecular recognition stage or a different relative spatial arrangement between each inhibitor and the reactive N-terminus, stemming from a ligand-specific pattern of favourable interactions with selected functional groups lying in the binding site.

The computational study was performed using the crystallographic structure of *bv*PLA_2 complexed with a phospholipid transition-state analogue, downloaded from the PDB (Protein Data Bank) archive (PDB code: 1 POC).[17] PM- and PR-PLA_2 complexes were obtained after replacing the phospholipid analogue with the inhibitors by manual docking PM (**1**) and PR (**5**), respectively, into the hydrophobic pocket of the protein, and then were submitted to an extensive docking search using the Affinity module[18,19] of InsightII (version 1998 and 2000.2, Accelrys, san Diego, USA). Fifty structures were collected and then further refined using the cell multipole method coupled with cycles of simulated annealing for more accurate results. A final energy minimization was carried out on every refined structure. Among the fifty inhibitor-PLA_2 molecular assemblies

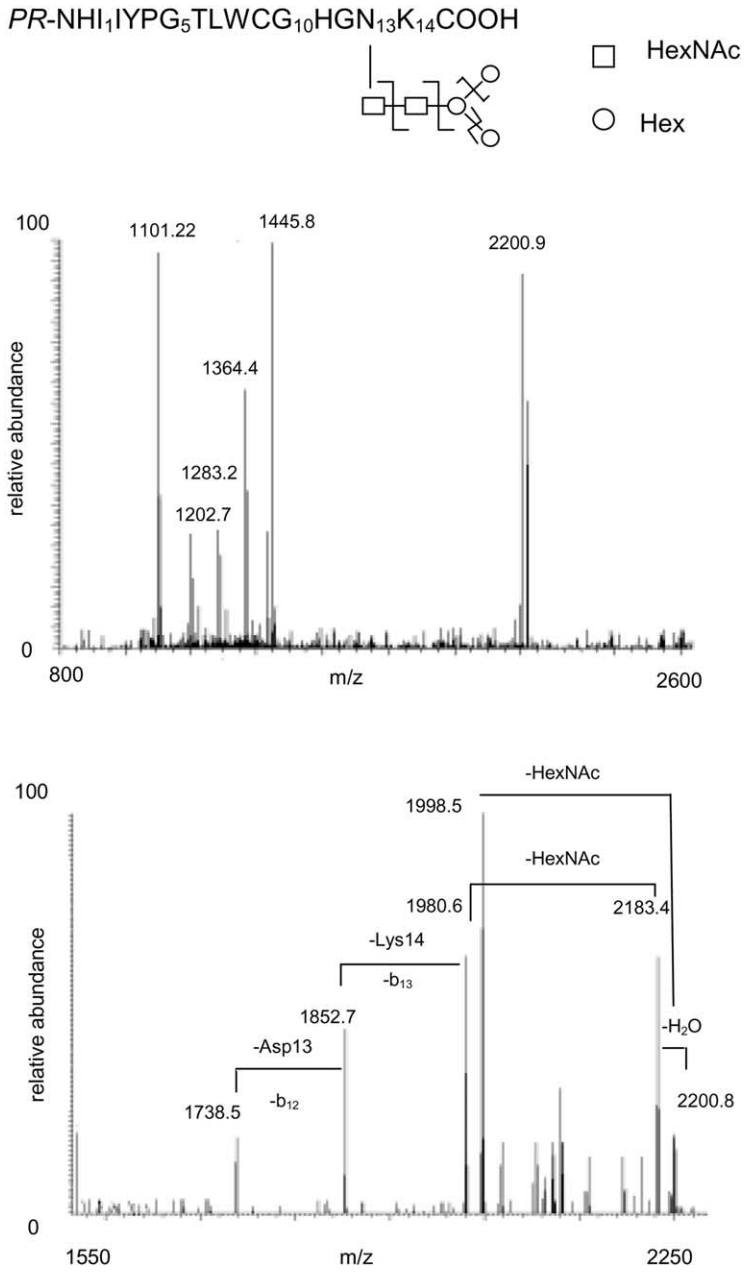

Figure 4. Upper panel: MS/MS spectrum of the doubly charged ion at m/z 1455.0. This ion species was attributed to the glycopeptide 1–14+ $HexNAc_2Hex_3$ monomodified by PR(**5**). The first fragment at m/z 1445.8 was generated by the loss of one molecule of water. Peaks at m/z 1364.4 ($HexNAc_2Hex_2$ glycopeptide), 1283.3 ($HexNAc_2Hex$ glycopeptide), 1202.7 ($HexNAc_2$ glycopeptide) and 1101.2 (HexNAc glycopeptide) corresponded to the sequential loss of three Hex residues and one HexNAc residue, respectively. The peak at m/z 2200.9 represented singly charged ion species of the 1–14 HexNAc fragment monomodified by PR (**5**). Lower panel: MS^3 spectrum obtained by the collision-induced dissociation of the singly charged species at m/z 2200.8 (HexNAc glycopeptide). The presence of b_{13} and b_{12} ions unequivocally indicated the Lys14 residue to be unmodified (see text).

obtained as output of our docking search, 20 structures used for final analysis were selected using our experimental data as logical constraints. Accordingly, only those 3D coordinates in which the location of the ligand inside the binding cleft was consistent with the possibility of a nucleophilic attack of the *bv*PLA_2 N-terminus to the C-25 of the 5-membered ring, were considered relevant. Analysis of the representative minimum energy structures showed significant differences for PM– and PR–PLA_2 complexes, as expected. In the case of PM (**1**), most structures display a common ligand orientation in which its reactive centre (the hemiacetalic C-25) is projected towards the amino terminal group (Ile-1) of the PLA_2 protein, suggesting that the recognition process alone ensures the correct positioning of the functional groups involved in the inactivation reaction (Schiff base formation). On the contrary, the lower degree of alignment in the inhibitor positioning found within the set of PR–PLA_2 assemblies, very likely arises from multiple favourable ligand arrangements in which the C-24 carboxylic group may be involved in electrostatic or hydrogen bonding interactions with various protein nitrogen atoms, including the N-terminus (Fig. 5). In other words, although PR may even possess a higher (non-covalent) affinity towards *bv*PLA_2 (as a consequence of strong electrostatic interactions), we believe that this greater structural dispersion in ligand positioning results in a much less effective covalent reactivity, as many of the observed inhibitor arrangements are incompatible with the covalent modification of the known reactive site of the enzyme.

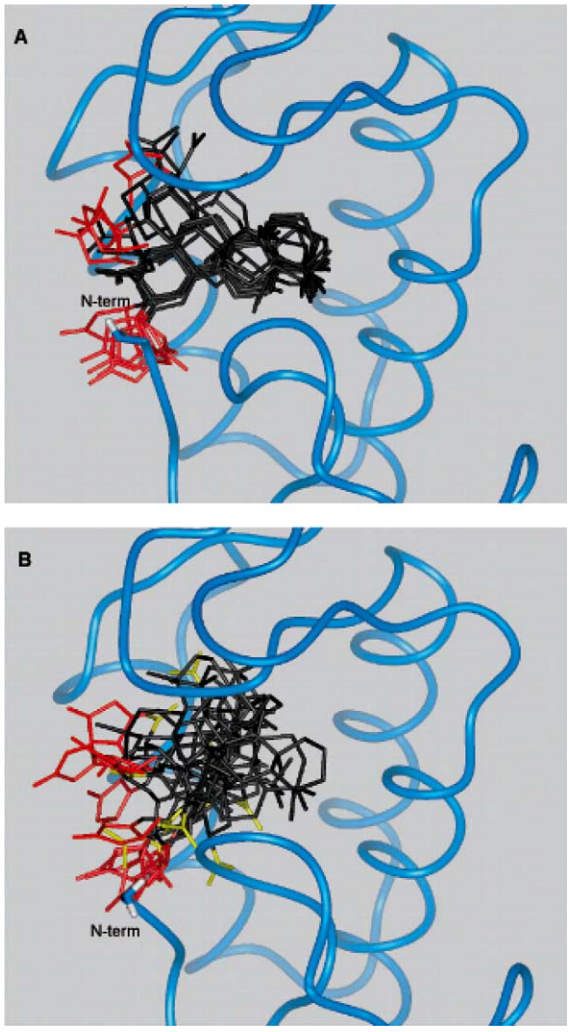

Figure 5. Representative selection of eight docked minimum energy structures of PM–PLA_2 (upper panel) and PR–PLA_2 (lower panel) adducts (see text and Experimental for details on the docking procedure). The protein backbone is represented by a blue ribbon. Amino acid side chains are omitted for clarity, except for N-terminal residue. The hydrophobic portion of petrosaspongiolides is represented by black sticks, γ-hydroxybutenolide moiety is coloured in red and C-24 carboxylic group of PR(**5**) in yellow.

3. Conclusion

A comparative analysis and a structural study on *bv*PLA_2 inactivation by different petrosaspongiolides were performed to validate the molecular mechanism proposed for PM[16] and to improve the comprehension of the molecular recognition stage between the enzyme and these marine sesterterpene inhibitors.

Based on our interpretation of the data, of pivotal importance for the inactivation process is the correct positioning of the ligand in the active site, induced by non-covalent interactions.

Starting from these results, and on the basis of a similar pharmacological profile,[2] a detailed investigation on human secretory PLA_2 inhibition processes by petrosaspongiolides is under way, with the purpose of a future rational design of simplified analogues as novel lead compounds for developing anti-inflammatory drugs.

4. Experimental

4.1. Preparation and analysis of the complexes between *bv*PLA_2 and Petrosaspongiolides M–R

Each inhibitor (PM-PR, **1**–**5**) was dissolved in isopropyl alcohol (1 mg/mL) and, one by one, added to a solution of *bv*PLA_2 (25 μM in 10 mM $Na_2B_4O_7$ at pH = 7.4) for 5 min at 40 °C with a 5:1 molar excess of natural product.

Then, the mixture was diluted with an equal volume of $NaBH_4$ (molar ratio $NaBH_4$: *bv*PLA_2 = 400:1) in NaOH (15 mM) for 2 h at 0 °C and the reaction was quenched adding 10 μL of a HCl 6M solution. The mixture was analysed by RP-HPLC on a Phenomenex C4 narrow-bore column by means a linear gradient from 25% to 95% aqueous acetonitrile containing 0.05% TFA, over 45 min. Elution profile was monitored at 220 and 280 nm. The fractions were collected and analyzed by an electrospray ion source at 220 °C at a flow rate of 5 μL/min on a Finnigan LCQ Deca ion trap mass spectrometer (ThermoQuest, San José, CA). Data were analyzed using the suite of programs Xcalibur (ThermoQuest, San José, CA), while the Magtran

software (Zhang and Marshall Zscore Algorithm) was used for data processing; all masses were reported as average values.

Integrations of HPLC peaks of unreacted protein were computed using the HPCHEM software (Agilent technologies, Germany). The percent of reacted protein was calculated after incubation with each petrosaspongiolide by means the following ratio: (area under peaks of *bv*PLA_2 prior incubation−area under peaks of *bv*PLA_2 unreacted after incubation)/(area under peaks of *bv*PLA_2 prior incubation)*100.

4.2. Structural analysis of the *bv*PLA_2–PR adduct

HPLC fractions containing unreacted protein and *bv*PLA_2–PR monomodified complex were dissolved in 200 μL of reduction buffer (guanidinium chloride 6M, tris(hydroxymethyl)aminomethane chloride 0.1M, sodium ethylenediaminotetraacetate 1 mM, pH 7,5) in the presence of DTT. The disulfide bond reduction was quenched after 2 h at 37 °C by a large excess of iodoacetamide. The alkylation of free cystenil groups was performed for 45 min at room temperature in the dark and stopped by acetic acid. Proteins were purified by a RP-HPLC and lyophilized.

Proteolysis experiments were performed on each sample, using endoproteinase Lys-C as hydrolytic probe, for 4 h at 37 °C and at a 1/50 (w/w) enzyme/substrate ratio. Digested peptides were eluted by RP-HPLC by means a linear gradient from 15% to 95% aqueous acetonitrile containing 0.05% TFA over 65 min on a C18 narrow-bore column. The fractions were manually collected and the peptides were analyzed by ESIMS and ESIMS/MS. CID (collision induced dissociation) MS/MS conditions were set with normalized collision energy of 30%.

4.3. Molecular modelling

All molecular modelling was performed on a Silicon Graphics Indigo 2 workstation equipped with a R10000 processor. Docking calculations were performed using the Affinity module of InsightII (versions 1998 and 2000.2, Accelrys Inc., San Diego, USA). The CVFF force field was used with standard parameters. The 3-D coordinates of *bv*PLA_2 were downloaded from the PDB archive (http://www.rcsb.org/pdb/ PDB code for bee venom PLA_2 crystallographic structure: 1POC). The input PR-PLA_2 and PM-PLA_2 complexes for Affinity calculations were generated by manually placing each inhibitor molecule into the *bv*PLA_2 hydrophobic pocket at the interface of the three α-helices, in the close proximity of the catalytic site. Then, an automatic docking search was performed on each of the so generated molecular assemblies by means a simulated annealing procedure. The following parameters were chosen for the docking search: the radius of the sphere representing the receptor binding site was set at 7 Å; the ligand was allowed to freely rotate and move within 2 Å from its original positioning; each of the ligand roteable bonds was given 180° of maximum freedom for its random changes during the simulation. For an initial sampling, a quartic repulsive potential was employed for treating non-bonding interactions, applying a scaling factor of 0.1. Fifty structures were collected and subsequently refined using the cell multipole method coupled with cycles of simulated annealing stages for more accurate results. A final energy minimization (1000 steps, conjugate gradient (Polak-Ribiere) algorithm) was carried out on each final structure. Twenty structures displaying a ligand orientation in agreement with experimental data, namely those with the pharmacophoric γ-hydroxubutenolide portion facing the outer, solvent exposed side of the binding pocket, in the proximity of the N-terminus, were selected for further analysis.

Acknowledgements

The University of Salerno and the Ministry of Instruction, University and Research (MIUR Rome) are gratefully acknowledged for financial support to this project through the funds ex-60% and PRIN 2001, 2003 programs, respectively.

References and notes

1. Soriente, A.; De Rosa, M.; Scettri, A.; Sodano, G.; Terencio, M. C.; Payà, M.; Alcaraz, M. J. *Curr. Med. Chem.* **1999**, *6*, 415.
2. Randazzo, A.; Debitus, C.; Minale, L.; Garcìa-Pastor, P.; Alcazar, M. J.; Payà, M.; Gomez-Paloma, L. *J. Nat. Prod.* **1998**, *61*, 571.
3. (a) Glaser, K. B.; De Carvalho, M.; Jacobs, R.; Kernan, M.; Faulkner, D. J. *Molecular Pharmacology* **1989**, *36*, 782. (b) Glaser, K. B.; Jacobs, R. *Biochemical Pharmacology* **1986**, *3*, 449.
4. Garcìa-Pastor, P.; Randazzo, A.; Gomez-Paloma, L.; Alcazar, M. J.; Payà, M. *J. Pharmacol. Exp. Ther.* **1999**, *289*, 166.
5. Much care must be taken with comparison of IC_{50} values of these PLA_2 irreversible blockers. IC_{50} values may vary as 100-fold depending on how long the enzyme is pre-incubated with the inhibitor. Therefore, data are fully comparable only when measured under the same experimental conditions.
6. Posadas, I.; Terencio, M. C.; Randazzo, A.; Gomez-Paloma, L.; Alcazar, M. J.; Payà, M. *Biochem. Pharmacology* **2003**, *65*, 887.
7. Vadas, P.; Pruzanski, W. *Laboratory Investigation* **1986**, *4*, 391.
8. Schevitz, R. W.; Bach, N. J.; Carlson, D. G.; Chirgadze, N. Y.; Clawson, D. K.; Dillaheim, R. D.; Draheim, S. E.; Hartley, L. W.; Jones, N. D.; Mihelich, E. D.; Olkowski, J. L.; Snyder, D. W.; Sommers, C.; Wery, J.-P. *Nature Structural Biology* **1995**, *2*, 458.
9. Parente, L. *The Journal of Rheumatology* **2001**, *28*, 2375.
10. Balsinde, J.; Balboa, M.; Insel, P.; Dennis, E. *Annu. Rev. Pharmacol. Toxicol.* **1999**, *39*, 175.
11. Lehr, M. *Export Opinion on Therapeutic Patents* **2001**, *11*, 1123.
12. Hansford, K. A.; Ried, R. C.; Clark, C. I.; Tyndall, J. D. A.; Whitehouse, M. W.; Guthrie, T.; McGeary, R. P.; Schafer, K.; Martin, J. L.; Fairlie, D. P. *ChemBiochem.* **2003**, *4*, 181.
13. Kokotos, G.; Kotsovolou, S.; Six, D. A.; Constantinou-Kokotou, V.; Beltzner, C. C.; Dennis, E. A. *J. Med. Chem.* **2002**, *45*, 2891.

14. Connoly, S.; Bennion, C.; Botterell, S.; Croshaw, P. J.; Hallam, C.; Hardy, K.; Hartopp, P.; Jackson, C. G.; King, S. J.; Lawrence, L.; Mete, A.; Murray, D.; Robinson, D. H.; Smith, G. M.; Stein, L.; Walters, I.; Wells, E.; Withnall, W. J. *J. Med. Chem.* **2002**, *45*, 1348.
15. Seno, K.; Okuno, T.; Nishi, K.; Murakami, Y.; Watanabe, F.; Matsuura, T.; Wada, M.; Fujii, Y.; Yamada, M.; Ogawa, T.; Okada, T.; Hashizume, H.; Kii, M.; Hara, S.-I.; Hagishita, S.; Nakamoto, S.; Yamada, K.; Chikazawa, Y.; Ueno, M.; Teshirogi, I.; Ono, T.; Ohtani, M. *J. Med. Chem.* **2000**, *43*, 1041.
16. Dal Piaz, F.; Casapullo, A.; Randazzo, A.; Riccio, R.; Pucci, P.; Marino, G.; Gomez-Paloma, L. *ChemBioChem.* **2002**, *3*, 664.
17. (a) Scott, D. J.; Otwinowski, Z.; Gelb, M. H.; Singer, P. B. *Science* **1990**, *250*, 1563. (b) Scott, D. J.; White, S. P.; Otwinowski, Z.; Yuan, W.; Gelb, M. H.; Singer, P. B. *Science* **1990**, *250*, 1541.
18. Carlson, H. A.; Cammon, J. A. *Molecular Pharmacology* **2000**, *57*, 213.
19. Wang, Z.; Canagarajah, B. J.; Bohem, J. C.; Kassisa, S.; Cobb, M. H. *Structure* **1998**, *6*, 1117.